Journal of Science and Technology in Civil Engineering NUCE 2018. 12 (3): 23–33

FREE VIBRATION ANALYSIS OF SANDWICH BEAMS WITH FG POROUS CORE AND FGM FACES RESTING ON WINKLER ELASTIC FOUNDATION BY VARIOUS SHEAR DEFORMATION THEORIES

Dang Xuan Hung[a,*], Huong Quy Truong[a]

[a] *Faculty of Building and Industrial Construction, National University of Civil Engineering, 55 Giai Phong road, Hai Ba Trung district, Hanoi, Vietnam*

Article history:
Received 02 March 2018, Revised 26 March 2018, Accepted 27 April 2018

Abstract

This paper studies the free vibration behavior of a sandwich beam resting on Winkler elastic foundation. The sandwich beam is composed of two FGM face layers and a functionally graded (FG) porous core. A common general form of different beam theories is proposed and the equations of motion are formulated using Hamilton's principle. The result of the general form is validated against those of a particular case and shows a good agreement. The effect of different parameters on the fundamental natural frequency of the sandwich beam is investigated.

Keywords: sandwich beam; FGM; functionally graded porous core; free vibration; natural frequency.

1. Introduction

Functionally graded (FG) porous material is a novel FGM in which porous property is characterized by the FG distribution of internal pores in the microstructure. Beside the common advantages of FGM materials, the FG porous materials also present excellent energy-absorbing capability. The advantages of this material type led to the development of many FG sandwich structures that have no interface problem as in the traditional laminated composites. These structures become even more attractive due to the introduction of FGMs for the faces and porous materials for the core. However, shear strength is always a disadvantage of this type of structures. Thus, a study of the effect of shear deformation on their behavior is necessary.

Based on great advantages of FG sandwich structures, many researchers have paid their attention to investigate mechanical behavior of these structures. Queheillalt et al. (2000) studied the creep expansion of porous sandwich structure in the process of hot rolling and annealing. In this process, the porous core of the sandwich material is produced by consolidating argon gas charged powder [1]. This

*Corresponding author. *E-mail address:* hungdx@nuce.edu.vn (Hung, D. X)

process was then simulated by the same authors in [2]. This idea was developed in the investigation of compression property of sandwich beam with porous core by [3]. Mechanical behaviour of sandwich structure with porous core is also interesting to the researchers. In 2006, Conde et al. investigated the sandwich beams with metal foam core and showed a significant saving of weight generated by the grading of porosity in the core in the yield-limited design [4]. The bending and forced vibration analysis of the same type of sandwich beam were respectively considered by [5, 6]. The buckling and free vibration analysis was more popular subject in numerous publications such as [6–9]. Specially Moschini in [10] studied the vibroacoustic modeling of the sandwich foam core panels.

The beam theories can be classified into two main categories. The first one is the equivalent single layer theory, which can be further divided into three groups. The first group based on the Taylor expansion of the displacement field and is called the shear deformation theory. It was used in numerous of studies and was reviewed in articles of [7, 9, 11, 12]. Another group uses the Carrera unified formulation (CUF) in which the displacement field is expanded on a generic function basis. This was used by Mashat and Filippi to study the mechanical behaviour of FGM beams in [12, 13]. The last group uses the parabolic or trigonometric type function to establish the displacement field and was reviewed in works of [7, 9, 14]. The second main category is the layerwise theory, in which the form of the displacement field of each layer is assumed differently. The application of this theory was detailed in [7, 9, 11, 14]. A special case of the layerwise theory that uses the zigzag type function to establish the different displacement field in the layers, was also used in [15].

This paper proposes a general form of displacement field for various single layer beam theories and establishes the equations of motion using Hamilton's principle. This general form of beam theories is then employed to investigate the fundamental natural frequency of the sandwich beam with FG core and FGM faces resting on Winkler elastic foundation, which, in our opinion, is less studied so far.

2. Sandwich beam with functionally graded porous core and FGM face layers

Consider a $L \times b \times h$ sandwich beam with the layers being numbered from bottom to top as shown in Fig. 1. The FG sandwich beam is composed of two FG face layers and an FG porous core. The top and bottom faces are at $z = \pm h/2$ coordinates. The beam is assumed to be placed on Winkler elastic foundation. It is numbered by layer thickness ratio from the bottom ($z = h_1 = -h/2$) to the top ($z = h_4 = +h/2$), e.g. a 1-1-1 FG sandwich beam is the beam that has equal thickness for every layer.

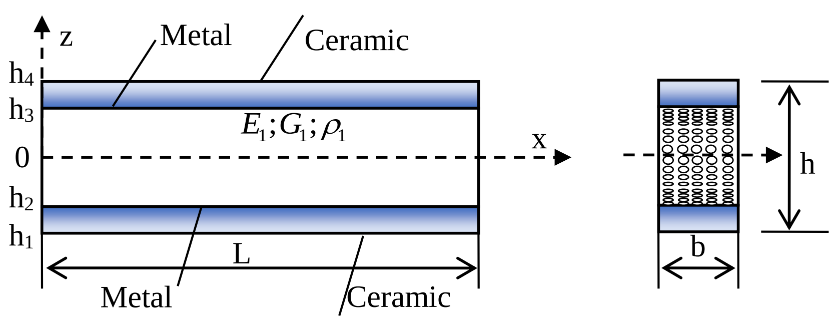

Figure 1. Sandwich beam with functionally graded porous core and FGM face layers

The Young's modulus of elasticity and the mass density of each layers vary through the thickness according to the following laws [8].

$$
\begin{aligned}
&E^{(3)}(z) = (E_c - E_m)\left(\frac{z-h_3}{h_4-h_3}\right)^p + E_m; \rho^{(3)}(z) = (\rho_c - \rho_m)\left(\frac{z-h_3}{h_4-h_3}\right)^p + \rho_m \quad \text{with} \quad z \in [h_3, h_4] \\
&E^{(2)}(z) = E_m\left[1 - e_0 \cos\left(\frac{\pi z}{h_3-h_2}\right)\right]; \rho^{(2)}(z) = \rho_m\left[1 - e_m \cos\left(\frac{\pi z}{h_3-h_2}\right)\right] \quad \text{with} \quad z \in [h_2, h_3] \\
&E^{(1)}(z) = (E_c - E_m)\left(\frac{z-h_1}{h_2-h_3}\right)^p + E_m; \rho^{(1)}(z) = (\rho_c - \rho_m)\left(\frac{z-h_1}{h_2-h_3}\right)^p + \rho_m \quad \text{with} \quad z \in [h_1, h_2]
\end{aligned}
\tag{1}
$$

where $E(z), \rho(z)$ are Young's modulus and mass density at z coordinate; E_m, ρ_m and E_c, ρ_c are Young's modulus and mass density respectively of metal and ceramic; e_0, e_m represent the coefficients of porosity and of mass density.

$$
e_0 = 1 - E_2/E_1, \quad e_m = 1 - \rho_2/\rho_1 \tag{2}
$$

with E_1, ρ_1 and E_2, ρ_2 are the maximum and minimum values of Young's modulus and of mass density of the porous core.

3. General form of shear deformation beam theories

3.1. Displacement field

The displacement field of the beam is assumed having the following general form.

$$
u(x,z,t) = u_0(x,t) + f_1(z)\frac{\partial w_0}{\partial x} + f_2(z)\theta_x, \quad w(x,z,t) = w_0(x,t) \tag{3}
$$

where u_0, w_0 are the in plane displacement components in the x, z directions; θ_x is the mid-plan rotation of transverse normal; $f_1(z), f_2(z)$ are the functions depending on the beam theory and shown in Table 1.

Table 1. Detail of functions $f_1(z), f_2(z)$ depending on the beam theory

Beam theory	Notation	$f_1(z)$	$f_2(z)$
Euler–Bernoulli	CBT	$-z$	0
Timoshenko	FSDBT	$-z$	z
Parabolic shear deformation beam theory [16]	PSDBT	$-z$	$z\left[1 - \frac{4}{3}\left(\frac{z}{h}\right)^2\right]$
Trigonometric shear deformation beam theory [14]	TSDBT	$-z$	$\frac{h}{\pi}\sin\left(\frac{\pi z}{h}\right)$
Exponential shear deformation beam theory [17]	ESDBT	$-z$	$ze^{-2(z/h)^2}$

3.2. Strain and stress fields

The strain field is obtained from the general displacement field using the following relations.

$$
\varepsilon_{xx} = \frac{\partial u}{\partial x} = \frac{\partial u_0}{\partial x} + f_1(z)\frac{\partial^2 w_0}{\partial x^2} + f_2(z)\frac{\partial \theta_x}{\partial x} \gamma_{xz} = \frac{\partial u}{\partial z} + \frac{\partial w}{\partial x} = \left(1 + f_1'(z)\right)\frac{\partial w_0}{\partial x} + f_2'(z)\theta_x \tag{4}
$$

The stress field in the i^{th} layer is determined from the strain field via the Hooke law, in which the coefficient of Poisson ν is assumed to be constant across the thickness of the beam.

$$\begin{Bmatrix} \sigma_{xx} \\ \sigma_{xz} \end{Bmatrix}^i = \begin{pmatrix} \dfrac{E(z)}{1-\nu^2} & 0 \\ 0 & \dfrac{K_s E(z)}{2(1+\nu)} \end{pmatrix}^i \begin{Bmatrix} \varepsilon_{xx} \\ \gamma_{xz} \end{Bmatrix}^i \tag{5}$$

where K_s is shear correction factor, $K_s = 5/6$ for Timoshenko theory and $K_s = 1$ otherwise.

3.3. Hamilton's principle and equations of motion

The Hamilton's principle is written as following.

$$\int_0^T (\delta U + \delta V - \delta K)dt = 0 \tag{6}$$

where δU, δV, δK are respectively first variation of virtual strain energy, of virtual work done by external forces and of virtual kinetic energy of the beam.

First variation of the virtual strain energy.

$$\begin{aligned}
\delta U &= \int_0^L \int_A (\sigma_{xx}\delta\varepsilon_{xx} + \sigma_{xz}\delta\gamma_{xz})\, dAdx \\
&= \int_0^L \int_A \left[\sigma_{xx}\delta\left(\frac{\partial u_0}{\partial x} + f_1(z)\frac{\partial^2 w_0}{\partial x^2} + f_2(z)\frac{\partial \theta_x}{\partial x}\right) + \sigma_{xz}\delta\left(\left(1 + f_1'(z)\right)\frac{\partial w_0}{\partial x} + f_2'(z)\theta_x\right)\right] dAdx \\
&= \int_0^L \left(N_{xx}\delta\left(\frac{\partial u_0}{\partial x}\right) + M_{xx}\delta\left(\frac{\partial^2 w_0}{\partial x^2}\right) + F_{xx}\delta\left(\frac{\partial \theta_x}{\partial x}\right) + Q_{xz}\delta\left(\frac{\partial w_0}{\partial x}\right) + H_{xz}\delta\theta_x\right)dx \\
&= \int_0^L \left(-\frac{\partial N_{xx}}{\partial x}\delta u_0 - \frac{\partial M_{xx}}{\partial x}\delta\left(\frac{\partial w_0}{\partial x}\right) - \frac{\partial F_{xx}}{\partial x}\delta\theta_x - \frac{\partial Q_{xz}}{\partial x}\delta w_0 + H_{xz}\delta\theta_x\right)dx \\
&\quad + N_{xx}\delta u_0\Big|_0^L + M_{xx}\delta\left(\frac{\partial w_0}{\partial x}\right)\Bigg|_0^L + F_{xx}\delta\theta_x\Big|_0^L + Q_{xx}w_0\Big|_0^L \\
&= \int_0^L \left(-\frac{\partial N_{xx}}{\partial x}\delta u_0 + \frac{\partial^2 M_{xx}}{\partial x^2}\delta w_0 - \frac{\partial F_{xx}}{\partial x}\delta\theta_x - \frac{\partial Q_{xz}}{\partial x}\delta w_0 + H_{xz}\delta\theta_x\right)dx \\
&\quad + N_{xx}\delta u_0\Big|_0^L + M_{xx}\delta\left(\frac{\partial w_0}{\partial x}\right)\Bigg|_0^L + F_{xx}\delta\theta_x\Big|_0^L + Q_{xx}w_0\Big|_0^L - \frac{\partial M_{xx}}{\partial x}\delta w_0\Bigg|_0^L
\end{aligned} \tag{7}$$

where

$$\begin{aligned}
N_{xx} &= \int_A \sigma_{xx}dA; \qquad M_{xx} = \int_A f_1(z)\sigma_{xx}dA; \qquad F_{xx} = \int_A f_2(z)\sigma_{xx}dA; \\
Q_{xz} &= \int_A \left(1 + f_1'(z)\right)\sigma_{xz}dA; \qquad H_{xz} = \int_A f_2'(z)\sigma_{xz}dA
\end{aligned} \tag{8}$$

- First variation of the virtual work done by external forces.

$$\delta V = -\int_0^L (q - k_n w_0)\,\delta w_0 dx \tag{9}$$

where q is distributed transverse load ($q = 0$ in this case) and k_n is Winkler foundation stiffness.

- First variation of the virtual kinetic energy.

$$\begin{aligned}
\delta K &= \int_0^L \int_A \rho(z)\,(\dot{u}\delta\dot{u} + \dot{w}\delta\dot{w})\,dAdx \\
&= \int_0^L \int_A \rho(z) \left[\left(\dot{u}_0 + f_1(z)\frac{\partial \dot{w}_0}{\partial x} + f_2(z)\dot{\theta}_x \right) \left(\delta\dot{u}_0 + f_1(z)\delta\left(\frac{\partial \dot{w}_0}{\partial x}\right) + f_2(z)\delta\dot{\theta}_x \right) + \dot{w}_0\delta\dot{w}_0 \right] dAdx \\
&= \int_0^L \int_A \rho(z) \left[\begin{array}{l} \dot{u}_0\delta\dot{u}_0 + f_1(z)\dot{u}_0\delta\left(\dfrac{\partial \dot{w}_0}{\partial x}\right) + f_2(z)\dot{u}_0\delta\dot{\theta}_x + f_1(z)\dfrac{\partial \dot{w}_0}{\partial x}\delta\dot{u}_0 + f_1^2(z)\dfrac{\partial \dot{w}_0}{\partial x}\delta\left(\dfrac{\partial \dot{w}_0}{\partial x}\right) \\ +f_1(z)f_2(z)\dfrac{\partial \dot{w}_0}{\partial x}\delta\dot{\theta}_x + f_2(z)\dot{\theta}_x\delta\dot{u}_0 + f_1(z)f_2(z)\dot{\theta}_x\delta\left(\dfrac{\partial \dot{w}_0}{\partial x}\right) + f_2^2(z)\dot{\theta}_x\delta\dot{\theta}_x + \dot{w}_0\delta\dot{w}_0 \end{array} \right] dAdx \\
&= \int_0^L \left(\begin{array}{l} I_0\dot{u}_0\delta\dot{u}_0 + I_1\dot{u}_0\delta\left(\dfrac{\partial \dot{w}_0}{\partial x}\right) + I_3\dot{u}_0\delta\dot{\theta}_x + I_1\dfrac{\partial \dot{w}_0}{\partial x}\delta\dot{u}_0 + I_2\dfrac{\partial \dot{w}_0}{\partial x}\delta\left(\dfrac{\partial \dot{w}_0}{\partial x}\right) \\ +I_4\dfrac{\partial \dot{w}_0}{\partial x}\delta\dot{\theta}_x + I_3\dot{\theta}_x\delta\dot{u}_0 + I_4\dot{\theta}_x\delta\left(\dfrac{\partial \dot{w}_0}{\partial x}\right) + I_5\dot{\theta}_x\delta\dot{\theta}_x + I_0\dot{w}_0\delta\dot{w}_0 \end{array} \right) dx \\
&= \int_0^L \left(\begin{array}{l} I_0\dot{u}_0\delta\dot{u}_0 - I_1\dfrac{\partial \dot{u}_0}{\partial x}\delta\dot{w}_0 + I_3\dot{u}_0\delta\dot{\theta}_x + I_1\dfrac{\partial \dot{w}_0}{\partial x}\delta\dot{u}_0 - I_2\dfrac{\partial^2 \dot{w}_0}{\partial x^2}\delta\dot{w}_0 \\ +I_4\dfrac{\partial \dot{w}_0}{\partial x}\delta\dot{\theta}_x + I_3\dot{\theta}_x\delta\dot{u}_0 - I_4\dfrac{\partial \dot{\theta}_x}{\partial x}\delta\dot{w}_0 + I_5\dot{\theta}_x\delta\dot{\theta}_x + I_0\dot{w}_0\delta\dot{w}_0 \end{array} \right) dx \\
&\quad + I_1\dot{u}_0\delta\dot{w}_0\big|_0^L + I_2\frac{\partial \dot{w}_0}{\partial x}\delta\dot{w}_0\bigg|_0^L + I_4\dot{\theta}_x\delta\dot{w}_0\big|_0^L
\end{aligned} \tag{10}$$

Substituting the expressions (7), (9) and (10) into equation (6) one obtains.

$$\begin{aligned}
0 &= \int_0^T \int_0^L \left(\begin{array}{l} -\dfrac{\partial N_{xx}}{\partial x}\delta u_0 + \dfrac{\partial^2 M_{xx}}{\partial x^2}\delta w_0 - \dfrac{\partial F_{xx}}{\partial x}\delta\theta_x - \dfrac{\partial Q_{xz}}{\partial x}\delta w_0 + H_{xz}\delta\theta_x + k_n w_0\delta w_0 \\ -I_0\dot{u}_0\delta\dot{u}_0 + I_1\dfrac{\partial \dot{u}_0}{\partial x}\delta\dot{w}_0 - I_3\dot{u}_0\delta\dot{\theta}_x - I_1\dfrac{\partial \dot{w}_0}{\partial x}\delta\dot{u}_0 + I_2\dfrac{\partial^2 \dot{w}_0}{\partial x^2}\delta\dot{w}_0 \\ -I_4\dfrac{\partial \dot{w}_0}{\partial x}\delta\dot{\theta}_x - I_3\dot{\theta}_x\delta\dot{u}_0 + I_4\dfrac{\partial \dot{\theta}_x}{\partial x}\delta\dot{w}_0 - I_5\dot{\theta}_x\delta\dot{\theta}_x - I_0\dot{w}_0\delta\dot{w}_0 \end{array} \right) dxdt \\
&\quad + \int_0^T \left(\begin{array}{c} N_{xx}\delta u_0\big|_0^L + M_{xx}\delta\left(\dfrac{\partial w_0}{\partial x}\right)\bigg|_0^L + F_{xx}\delta\theta_x\big|_0^L + Q_{xx}\delta w_0\big|_0^L - \dfrac{\partial M_{xx}}{\partial x}\delta w_0\bigg|_0^L \\ -I_1\dot{u}_0\delta\dot{w}_0\big|_0^L - I_2\dfrac{\partial \dot{w}_0}{\partial x}\delta\dot{w}_0\bigg|_0^L - I_4\dot{\theta}_x\delta\dot{w}_0\big|_0^L \end{array} \right) dt \\
&= \int_0^T \int_0^L \left(\begin{array}{l} -\left(\dfrac{\partial N_{xx}}{\partial x} - I_0\ddot{u}_0 - I_1\dfrac{\partial \ddot{w}_0}{\partial x} - I_3\ddot{\theta}_x\right)\delta u_0 \\ +\left(\dfrac{\partial^2 M_{xx}}{\partial x^2} - \dfrac{\partial Q_{xz}}{\partial x} + k_n w_0 - I_1\dfrac{\partial \ddot{u}_0}{\partial x} - I_2\dfrac{\partial^2 \ddot{w}_0}{\partial x^2} - I_4\dfrac{\partial \ddot{\theta}_x}{\partial x} + I_0\ddot{w}_0\right)\delta w_0 \\ -\left(\dfrac{\partial F_{xx}}{\partial x} - H_{xz} - I_3\ddot{u}_0 - I_4\dfrac{\partial \ddot{w}_0}{\partial x} - I_5\ddot{\theta}_x\right)\delta\theta_x \end{array} \right) dxdt \\
&\quad + \int_0^T \left(\begin{array}{l} N_{xx}\delta u_0\big|_0^L + M_{xx}\delta\left(\dfrac{\partial w_0}{\partial x}\right)\bigg|_0^L + F_{xx}\delta\theta_x\big|_0^L + \left(Q_{xx} - \dfrac{\partial M_{xx}}{\partial x}\right)\delta w_0\bigg|_0^L \\ -\left(I_1\dot{u}_0 + I_2\dfrac{\partial \dot{w}_0}{\partial x} + I_4\dot{\theta}_x\right)\delta\dot{w}_0\bigg|_0^L \end{array} \right) dt
\end{aligned} \tag{11}$$

where

$$\begin{aligned} I_0 &= \int_A \rho(z)dA; \qquad I_1 = \int_A f_1(z)\rho(z)dA; \qquad I_2 = \int_A f_1^2(z)\rho(z)dA \\ I_3 &= \int_A f_2(z)\rho(z)dA; \qquad I_4 = \int_A f_1(z)f_2(z)\rho(z)dA; \qquad I_5 = \int_A f_2^2(z)\rho(z)dA \end{aligned} \tag{12}$$

The equations of motion are formulated by taking Euler-Lagrange equations from (11).

$$\begin{aligned} \delta u_0 &: \quad \frac{\partial N_{xx}}{\partial x} = I_0\ddot{u}_0 + I_1\frac{\partial \ddot{w}_0}{\partial x} + I_3\ddot{\theta}_x \\ \delta w_0 &: \quad \frac{\partial^2 M_{xx}}{\partial^2 x} - \frac{\partial Q_{xz}}{\partial x} + k_n\ddot{w}_0 = I_1\frac{\partial \ddot{u}_0}{\partial x} + I_2\frac{\partial^2 \ddot{w}_0}{\partial^2 x} + I_4\frac{\partial \ddot{\theta}_x}{\partial x} - I_0\ddot{w}_0 \\ \delta \theta_x &: \quad \frac{\partial F_{xx}}{\partial x} - H_{xz} = I_3\ddot{u}_0 + I_4\left(\frac{\partial \ddot{w}_0}{\partial x}\right) + I_5\ddot{\theta}_x \end{aligned} \tag{13}$$

3.4. Navier's solution

Navier's solution satisfies the boundary conditions of a simply supported beam and has the following form with $\alpha = n\pi/L$.

$$u_0 = \sum_{n=1}^{\infty} u_n \cos(\alpha x)\cos(\omega t)\,; \quad w_0 = \sum_{n=1}^{\infty} w_n \sin(\alpha x)\cos(\omega t)\,; \quad \theta_x = \sum_{n=1}^{\infty} \theta_n \cos(\alpha x)\cos(\omega t) \tag{14}$$

Take into account each term of the serie solution as a free vibration mode shape of the beam and replace it into the equations (3), (8) and (13), one obtains the eigenvalue-equations of the free vibration.

$$\left(\begin{bmatrix} k_{11} & k_{12} & k_{13} \\ k_{21} & k_{22} & k_{23} \\ k_{31} & k_{32} & k_{33} \end{bmatrix} - \omega^2 \begin{bmatrix} m_{11} & m_{12} & m_{13} \\ m_{21} & m_{22} & m_{23} \\ m_{31} & m_{32} & m_{33} \end{bmatrix}\right)\begin{pmatrix} u_n \\ w_n \\ \theta_n \end{pmatrix} = \begin{bmatrix} 0 \\ 0 \\ 0 \end{bmatrix} \tag{15}$$

4. Numerical results

Consider a simply supported FG sandwich beam of dimensions $L \times 1 \times h$ with metal foam core of porosity coefficient e_0 and FGM face layers. The FG sandwich beam is made of aluminum as metal (Al: $E_m = 70$ GPa, $\nu_m = 0,3$) and of Alumina as ceramic (Al_2O_3: $E_c = 380$ GPa, $\nu_c = 0,3$). The beam rests on a Winkler elastic foundation of constant k_n. Non-dimensional fundamental natural frequency is defined as [18].

$$\overline{\omega} = \frac{\omega L^2}{h}\sqrt{\frac{\rho_m}{E_m}} \tag{16}$$

4.1. Validation

In order to verify the accuracy of present study, a simply supported FG sandwich beam with isotropic core ($e_0 = 0$) without elastic foundation ($k_n = 0$) is considered. The non-dimensional fundamental natural frequencies are calculated for different face-core-face thickness ratios, two slenderness ratios $L/h = 5$; 20 and power law index $p = 5$ using various beam theories.

The results are compared with those obtained using refined shear deformation beam theory (RSDBT) of [18] and are presented in Table 2. It can be seen that non-dimensional fundamental natural frequencies of the parabolic shear deformation beam theory (PSDBT) are absolutely in agreement with that of RSDBT theory in [18]. The other theories show a good agreement with RSDBT except CBT and FSDBT show a little discrepancy.

Table 2. Comparison of non-dimensional fundamental natural frequencies of FG sandwich beam with isotropic core for various beam theories and beam configurations

p	Theory	$L/h = 5$				$L/h = 20$			
		1-0-1	2-1-2	1-1-1	1-2-1	1-0-1	2-1-2	1-1-1	1-2-1
5	RSDBT [18]	2.7446	2.8439	3.0181	3.3771	2.8439	2.9310	3.1111	3.4921
	PSDBT	2.7446	2.8439	3.0181	3.3771	2.8439	2.9310	3.1111	3.4921
	CBT	2.8082	2.8953	3.0741	3.4517	2.8483	2.9346	3.1149	3.4972
	FSDBT	2.7274	2.8281	3.0039	3.3652	2.8427	2.9299	3.1101	3.4913
	TSDBT	2.7462	2.8451	3.0188	3.3772	2.8440	2.9311	3.1111	3.4921
	ESDBT	2.7480	2.8463	3.0197	3.3773	2.8442	2.9312	3.1112	3.4921

4.2. Effect of slenderness ratio L/h

Consider a 1-2-1 sandwich FG beam consist metal foam core and FGM faces resting on Winkler elastic foundation with $e_0 = 0.4$, $p = 5$, $k_n = 10^7$ (N/m^3) and with different ratios $L/h = 5; 10; 15; 20; 30; 40$. The non-dimensional fundamental natural frequencies of the FG sandwich beam are presented in Table 3 and their variation versus slenderness ratios are graphically depicted in Fig. 2.

Table 3. Non-dimensional fundamental natural frequency $\overline{\omega}$ of 1-2-1 FG sandwich beam with different slenderness ratios

	Theory	L/h					
		5	10	15	20	30	40
$\overline{\omega}$	CBT	5.5914	5.7047	5.8538	6.2048	7.9592	11.4091
	FSDBT	5.1969	5.5910	5.8030	6.1775	7.9496	11.4054
	PSDBT	4.9243	5.5012	5.7615	6.1551	7.9417	11.4023
	TSDBT	4.8894	5.4889	5.7558	6.1519	7.9406	11.4018
	ESDBT	4.8542	5.4762	5.7498	6.1487	7.9395	11.4014

It is observed that the non-dimensional natural frequency increases with increasing value of slenderness ratios for all beam theories. When the ratio L/h is small, natural frequencies obtained by various theories are considerably different and they are more and more convergent when L/h increases. This result shows important effect of the shear deformation on the short beams.

4.3. Effect of the face-core-face thickness ratios

A sandwich beam with $L/h = 5$, $e_0 = 0.4$, $p = 5$, $k_n = 10^7$ (N/m^3) and different face-core-face thickness ratios is studied. The non-dimensional fundamental natural frequencies are presented in Table 4. Fig. 3 shows their variation with respect to face-core-face thickness ratios. It can be seen that, in most case, non-dimensional fundamental natural frequency decreases as the face-core-face thickness ratio increases. This can be explained by the reduction of bending stiffness of the beam when the porous core thickness increases. Nonetheless, when the thickness of the core is small (1-0-1 to 3-4-3), it seems that the frequency slightly increases in two cases: CBT, FSDBT. This is due to the low effect of shear deformation in these theories.

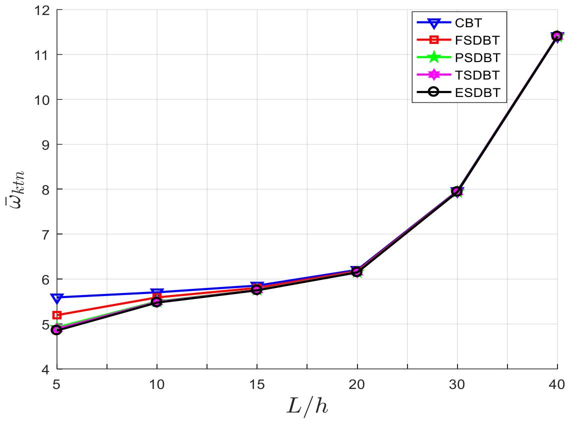

Figure 2. Effect of L/h ratio on non-dimensional natural frequency $\overline{\omega}$ of 1-2-1 sandwich beam

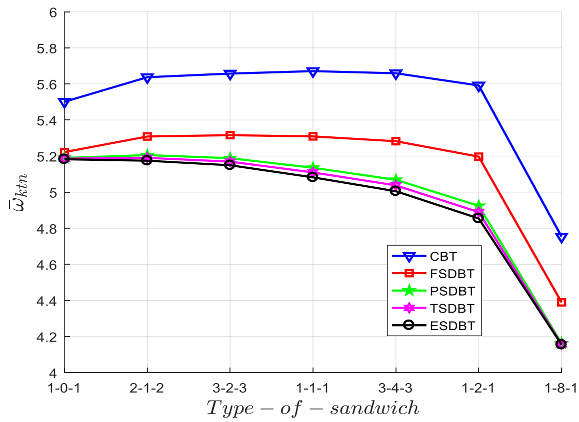

Figure 3. Effect of the face-core-face thickness ratio on non-dimensional fundamental natural frequency $\overline{\omega}$ of FG sandwich beams

Table 4. Non-dimensional natural frequency $\overline{\omega}$ of sandwich beams with different face-core-face thickness ratios

	Theory	Ratio of the layer's depth						
		1-0-1	2-1-2	3-2-3	1-1-1	3-4-3	1-2-1	1-8-1
$\overline{\omega}$	CBT	5.5009	5.6371	5.6572	5.6708	5.6590	5.5914	4.7538
	FSDBT	5.2220	5.3085	5.3158	5.3090	5.2824	5.1969	4.3892
	PSDBT	5.1898	5.2054	5.1883	5.1353	5.0684	4.9243	4.1615
	TSDBT	5.1858	5.1901	5.1692	5.1094	5.0375	4.8894	4.1568
	ESDBT	5.1824	5.1743	5.1491	5.0820	5.0052	4.8542	4.1551

4.4. Effect of volume fraction of FG face layers

Reconsider the 1-2-1 FG sandwich beam with $L/h = 5$, $e_0 = 0.4$, $k_n = 10^7$ (N/m^3) and different volume fraction indices of the face layers $p = 0.1; 0.5; 1; 2; 5; 10$. The obtained non-dimensional fundamental natural frequencies $\overline{\omega}$ of the beams are tabulated in Table 5. Fig. 4 exhibits the their variation with respect to volume fraction index of the face layers. As can be seen from the presented results, the non-dimensional natural frequency increases with increasing value of volume fraction index p of face layers. It is basically due to the fact that Young's modulus of ceramic is higher than those of metal. When the volume fraction p increases, the ceramic amount increases and this makes augment to natural frequency. The effect of shear deformation on the considered beams is also indicated in the figure.

4.5. Effect of porosity coefficient of the porous core

The non-dimensional fundamental natural frequencies computed for a 1-2-1 sandwich beam with $L/h = 5$, $p = 5$, $k_n = 10^7$ (N/m^3) and different values of porosity coefficient of the porous core $e_0 = 0; 0.2; 0.4; 0.6; 0.8$ to show the effect of this parameter. The results are presented in Table 6. The variation of non-dimensional fundamental natural frequencies versus porosity coefficients is illustrated in the Fig. 5. The presented results show that non-dimensional natural frequency of the

Table 5. Non-dimensional fundamental natural frequency $\overline{\omega}$ of FG sandwich beams with different values of volume fraction index of face layers

	Theory	Volume fraction index of the face layers p					
		0.1	0.5	1	2	5	10
$\overline{\omega}$	CBT	3.4579	4.5084	4.9964	5.3520	5.5914	5.6628
	FSDBT	3.2545	4.1951	4.6374	4.9664	5.1969	5.2700
	PSDBT	3.2120	4.0441	4.4182	4.7030	4.9243	5.0071
	TSDBT	3.2095	4.0341	4.3999	4.6754	4.8894	4.9706
	ESDBT	3.2078	4.0257	4.3833	4.6490	4.8542	4.9330

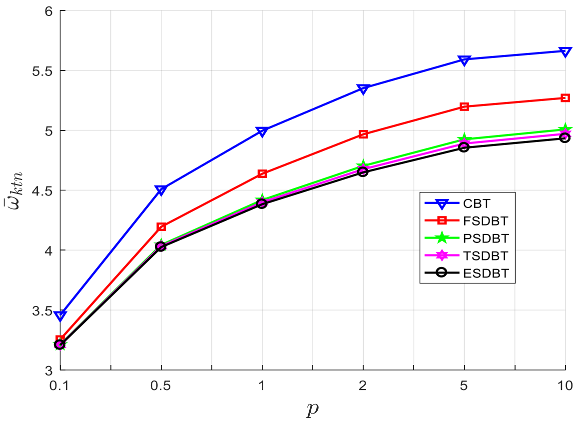

Figure 4. Effect of volume fraction index p of the face layers on non-dimensional fundamental natural frequency $\overline{\omega}$ of FG sandwich beams

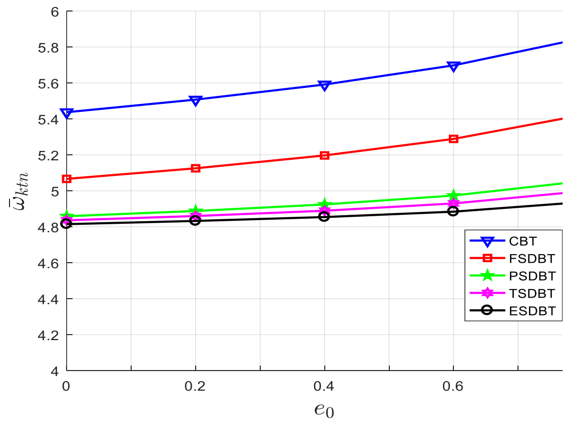

Figure 5. Effect of porosity coefficient of the porous core e_0 on non-dimensional natural frequency $\overline{\omega}$ of FG sandwich beams

Table 6. Non-dimensional fundamental natural frequency $\overline{\omega}$ of FG sandwich beams with different values of porosity coefficient of the porous core

	Theory	Porosity coefficient of the porous core e_0				
		0	0.2	0.4	0.6	0.8
$\overline{\omega}$	CBT	5.4373	5.5074	5.5914	5.6979	5.8487
	FSDBT	5.0666	5.1254	5.1969	5.2889	5.4219
	PSDBT	4.8587	4.8879	4.9243	4.9739	5.0539
	TSDBT	4.8361	4.8599	4.8894	4.9299	4.9978
	ESDBT	4.8148	4.8326	4.8542	4.8842	4.9375

beam increases with the increasing porosity coefficient. This seems reasonless because the increase of the porosity of the core will entrain the reduction of the bending stiffness of the beams and makes decrease the natural frequency. But one has to notice that this increase of the porosity also entrains the reduction of the mass density and its effect is inverse. Thus, combination of these two effects makes increase the natural frequency of the beam.

4.6. Effect of Winkler foundation stiffness

Consider a 1-2-1 sandwich beam with $L/h = 5$, $e_0 = 0.4$, $p = 5$ and different Winkler elastic foundation stiffness $k_n = 0.5; 20; 200; 500; 1000; 2000 \quad (\times 10^6 \quad \mathrm{N/m^3})$. The results presented in Table 7 and in Fig. 6. This figure shows that the non-dimensional fundamental natural frequency of the beam increases with the increasing constant of the elastic foundation. Because when the constant k_n increases, it makes augment to the bending stiffness of the beam and therefore entrains the increase of the natural frequency. Moreover we can also clearly observe the effect of the shear deformation as in the above other tests.

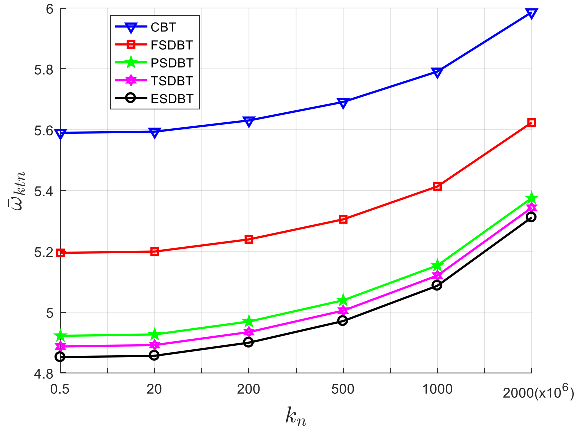

Figure 6. Effect of stiffness of Winkler elastic foundation k_n on non-dimensional natural frequency $\overline{\omega}$ of sandwich beams

Table 7. Non-dimensional natural frequency $\overline{\omega}$ of sandwich beams with increasing constant of Winkler elastic foundation obtained by various theories

	Theory	$k_n(\times 10^6$ N/m$^3)$					
		0.5	20	200	500	1000	2000
$\overline{\omega}$	CBT	5.5895	5.5935	5.6303	5.6911	5.7911	5.9860
	FSDBT	5.1948	5.1992	5.2392	5.3051	5.4133	5.6234
	PSDBT	4.9221	4.9267	4.9691	5.0390	5.1535	5.3750
	TSDBT	4.8871	4.8918	4.9345	5.0050	5.1202	5.3433
	ESDBT	4.8519	4.8566	4.8997	4.9707	5.0868	5.3114

5. Conclusions

This paper investigates the free vibration of sandwich beams with FG porous core and FGM faces resting on Winkler elastic foundation. A general form of the displacement field and the equations of motion through Hamilton's principle have been established. Using this general form of various beam theories, the paper shows the important effect of shear deformation on the fundamental natural frequency of short beams. The effects of Winkler foundation stiffness, transverse shear deformation, slenderness ratio, face-core-face thickness ratio, volume fraction index, as well as porosity coefficient of the core on the fundamental natural frequency are also investigated. The results show an inverse effect of the increase of porosity coefficient of the core on the fundamental natural frequency because of the reduction of the mass density.

References

[1] Queheillalt, D. T., Wadley, H. N. G., Choi, B. W., and Schwartz, D. S. (2000). Creep expansion of porous Ti-6Al-4V sandwich structures. *Metallurgical and Materials transactions A*, 31(1):261–273.

[2] Vancheeswaram, R., Queheillalt, D. T., Elzey, D. M., and Wadley, H. N. G. (2001). Simulation of the creep expansion of porous sandwich structures. *Metallurgical and Materials Transactions A*, 32(7):1813–1821.

[3] Bang, S. O. and Cho, J. U. (2015). A study on the compression property of sandwich composite with porous core. *International Journal of Precision Engineering and Manufacturing*, 16(6):1117–1122.

[4] Conde, Y., Pollien, A., and Mortensen, A. (2006). Functional grading of metal foam cores for yield-limited lightweight sandwich beams. *Scripta Materialia*, 54(4):539–543.

[5] Magnucka-Blandzi, E. and Magnucki, K. (2007). Effective design of a sandwich beam with a metal foam core. *Thin-Walled Structures*, 45(4):432–438.

[6] Bui, T. Q., Khosravifard, A., Zhang, C., Hematiyan, M. R., and Golub, M. V. (2013). Dynamic analysis of sandwich beams with functionally graded core using a truly meshfree radial point interpolation method. *Engineering Structures*, 47:90–104.

[7] Sayyad, A. S. and Ghugal, Y. M. (2015). On the free vibration analysis of laminated composite and sandwich plates: A review of recent literature with some numerical results. *Composite Structures*, 129: 177–201.

[8] Chen, D., Kitipornchai, S., and Yang, J. (2016). Nonlinear free vibration of shear deformable sandwich beam with a functionally graded porous core. *Thin-Walled Structures*, 107:39–48.

[9] Sayyad, A. S. and Ghugal, Y. M. (2017). Bending, buckling and free vibration of laminated composite and sandwich beams: A critical review of literature. *Composite Structures*, 171:486–504.

[10] Moschini, S. (2014). *Vibroacoustic modeling of sandwich foam core panels*. PhD thesis, Politecnico Di Milano, Italy.

[11] Hajianmaleki, M. and Qatu, M. S. (2013). Vibrations of straight and curved composite beams: A review. *Composite Structures*, 100:218–232.

[12] Mashat, D. S., Carrera, E., Zenkour, A. M., Al Khateeb, S. A., and Filippi, M. (2014). Free vibration of FGM layered beams by various theories and finite elements. *Composites Part B: Engineering*, 59: 269–278.

[13] Filippi, M., Carrera, E., and Zenkour, A. M. (2015). Static analyses of FGM beams by various theories and finite elements. *Composites Part B: Engineering*, 72:1–9.

[14] Ghugal, Y. M. and Shimpi, R. P. (2001). A review of refined shear deformation theories for isotropic and anisotropic laminated beams. *Journal of Reinforced Plastics and Composites*, 20(3):255–272.

[15] Gherlone, M. (2013). On the use of zigzag functions in equivalent single layer theories for laminated composite and sandwich beams: a comparative study and some observations on external weak layers. *Journal of Applied Mechanics*, 80(6):061004.

[16] Pradhan, K. K. and Chakraverty, S. (2014). Effects of different shear deformation theories on free vibration of functionally graded beams. *International Journal of Mechanical Sciences*, 82:149–160.

[17] Karama, M., Afaq, K. S., and Mistou, S. (2003). Mechanical behaviour of laminated composite beam by the new multi-layered laminated composite structures model with transverse shear stress continuity. *International Journal of Solids and Structures*, 40(6):1525–1546.

[18] Vo, T. P., Thai, H. T., Nguyen, T. K., Maheri, A., and Lee, J. (2014). Finite element model for vibration and buckling of functionally graded sandwich beams based on a refined shear deformation theory. *Engineering Structures*, 64:12–22.